Int J Clin Exp Med 2021;14(2):779-788
www.ijcem.com /ISSN:1940-5901/IJCEM0117247

Original Article

Predicting the effects of a distal femoral cartilage defect using an accurate three-dimensional dynamic finite element model

Lin-Song Ji[1], Yan-Lin Li[3], Yan-Ping Wang[2], Chun-Shan Luo[1], Lu Tong[3]

Departments of [1]Spine Surgery, [2]Gastroenterology, Guizhou Province Orthopedic Hospital, Guiyang, China; [3]Department of Sports Medicine, The First Affiliated Hospital of Kunming Medical University, Kunming, China

Received June 30, 2020; Accepted November 2, 2020; Epub February 15, 2021; Published February 28, 2021

Abstract: Objectives: The present study aimed to investigate how variables associated with an osteochondral femur defect affect tibiofemoral contact using three-dimensional (3D) finite element analysis. Methods: We reconstructed a 3D finite element model of a human knee joint, including the bone structure, cartilage, meniscus and tendons. Then, we built an 8-mm-diameter defect on the weight-bearing area of femoral condyle cartilage in finite element mode. At various flexion angles ranging from 0° to 90°, a 350-N vertical tibial plateau load and a 400-N traction force in the quadriceps direction were applied to the unconstrained proximal femur. After constructing the 3D model, Abaqus software was used for finite element analyses and calculations to examine the effect of an 8-mm defect in the medial femoral condyle (high-weight-bearing region) on the stress of the cartilage and meniscus at 0°, 30°, 60°, and 90° of knee flexion. Results: The results indicated that the forces in the tibiofemoral knee joint increased obviously at 0°, 30°, and 60° of knee flexion during compressive loading. However, at a flexion angle of 90°, the difference in peak stress was not statistically significant. Conclusion: This study demonstrated a significant increase in compressive stresses in the femoral cartilage, meniscus, and tibial cartilage with an 8-mm defect in the medial femoral condyle at 0°, 30°, 60°, and 90° of knee flexion. The present findings provide a better understanding of degenerative arthritis.

Keywords: Articular cartilage, biomechanics, finite element analysis, knee joint

Introduction

Focal chondral or osteochondral defects present several medical and personal complications; these defects can be painful and disabling and may contribute to the development of degenerative arthritis [1, 2]. Moreover, these defects have a markedly poor capacity for self-repair or even medically assisted repair and are the most common forms of trauma among young and active patients [3]. Clearly, better preventive and therapeutic techniques should be developed, but a lack of understanding of knee joint biomechanics impedes the development of these techniques [4, 5]. Despite several investigations, the specific mechanical behaviour of the knee joint and reasons for injuries remain unclear. To date, many experiments have demonstrated that finite element models (FEMs) can provide profound insights into the mechanical properties of biological tissues, overcoming the recurring obstacles of high time and cost requirements. An effectively developed FEM serves as an incredible asset to anticipate the impacts of various parameters involved, yielding information that is difficult to obtain from tests [6].

We aimed to use an accurate three-dimensional (3D) model of a healthy human knee joint including the patellar tendon [PT], anterior cruciate ligament [ACL], posterior cruciate ligament [PCL], medial collateral ligament [MCL], lateral collateral ligament [LCL], menisci, and articular cartilages. This model can demonstrate articular cartilage and meniscus pressure distributions in locations similar to cartilage defects on imaging studies. The primary

Table 1. Material mechanical properties of the femur, tibia, cartilage, and meniscus

	Elastic modulus (MPa)	Poisson's ratio
Femur	3883.4	0.3
Tibia	4184.6	0.3
Cartilage	20	0.46
Meniscus	59	0.49
MCL	467	0.46
LCL	467	0.46

Table 2. Material parameters of ligaments

	C_1	D
MCL	1.44	0.00126
LCL	1.44	0.00126
ACL	1.95	0.00683
PCL	3.25	0.0041
PT	2.75	0.00484

goal of developing this model was to determine the extent to which an osteochondral defect in the weight-bearing region of the femoral condyle influences the contact conduct of the knee joint during compressive stress loading. The findings may offer some insights into advancing cartilage defect repair.

Material and methods

Three-dimensional model and material properties

An accurate three-dimensional (3D) model of the left knee of a 25-year-old healthy male (height, 1.78 m; weight, 70 kg) was reconstructed based on magnetic resonance imaging (MRI) data. The following associated grouping and parameters were utilized: T1-weighted fat-suppressed gradient recall; repetition time, 11,000 ms; echo time, 25 ms; matrix size, 192/320; and slice thickness, 1.0 mm. MRI images were processed using Mimics 14.11 (Materialise, Leuven, Belgium) and Geomagic Studio 2012 (MSC Corporation, NC, USA) to construct the accurate three-dimensional model [7]. The model was then imported and meshed in Abaqus 6.9 (Simulia, RI, USA).

The model developed in this study incorporated data from previous reports defining bone, cartilage, meniscus, and ligaments as material properties [8]. Femoral cartilage, menisci, and tibial cartilage were presumed to act as linear elastic materials [8]. The elastic modulus for the incompressible matrix of menisci was 59 MPa with a Poisson's ratio of 0.49 [9]. The elastic modulus for the cartilage was 20 MPa with a Poisson's ratio of 0.46 as reported in previous joint model studies [10]. All ligaments were assumed to function as hyperelastic material. The constitutive relations model of the material was the neo-Hookean model (**Tables 1** and **2**). The neo-Hookean function was evaluated as follows [11]:

$$\psi = \frac{1}{2D}\ln(J)^2 + C_1(\bar{I}_1 - 3) + F_2(\lambda)$$

where C_1 is a neo-Hookean constant, and D is the bulk modulus.

Each tissue of the knee joint was meshed individually. The cartilage, ligaments, and menisci were all divided by tetrahedral solid units. The grid size was set to 1 mm, and the unit was set to a full integration unit. To allow comparisons of the clinical results of the present model with the findings of Yang [12] and Darryl [13], we modelled the smooth, frictionless contact surfaces between the femoral condyle cartilage and the tibial plateau cartilage, the femur and the meniscus articular surface, and the tibial and meniscus articular surface. Given the large elastic modulus of the subchondral bone, it had no significant impact on the calculation and analysis. The subchondral bone was not clearly defined, and the subchondral bone was regarded as a rigid body.

Loads

According to arthroscopic studies, approximately 60% of focal defects are located in the femoral cartilage, and more than half of focal defects in the femoral cartilage occur in the medial femoral condyle [14]. Thus, we created a model of an 8-mm defect in the medial femoral condyle. After constructing the 3D model, Abaqus software was used for finite element analysis and calculations to examine the effect of an 8-mm defect in the medial femoral condyle (high-weight-bearing regions) on the compressive stresses in the articular cartilage and meniscus at 0°, 30°, 60°, and 90° of knee flexion. A 350-N vertical tibial plateau load and a 400-N traction force in the quadriceps direc-

Figure 1. The total knee 3D digital geometric model. A. Back view. B. Lateral view.

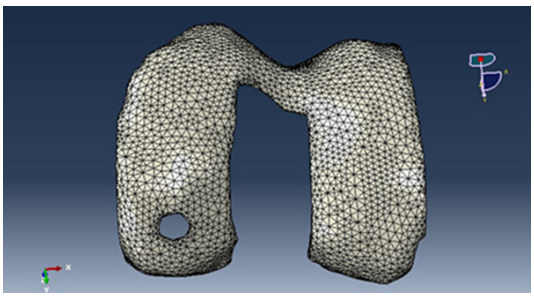

Figure 2. 3D digital finite element model of the cartilage defect in the medial femoral condyle.

tion (corresponding to 50% of the body weight) were applied in the knee joint model [15]. In this analysis, the distal tibia and fibula were completely restrained and fixed, while the femur was completely free without any constraints. A Von Mises equivalent stress nephogram was used to predict the peak stress of the articular cartilage and meniscus.

Statistical analysis

Data were recorded as the mean ± SD and analysed using SPSS 22.0 (SPSS, IL, USA). A *t*-test with two independent samples was performed. ($P < 0.05$) indicates a significant difference.

Results

The model of the knee joint retained its significant individual features. The model with bone and ligament was very similar to the exact anatomy and mirrored their separate anatomical shapes (**Figure 1**).

When applying a 400-N quadriceps load and a 350-N axial load on the distal femur, peak stresses were found in each part of the cartilage and meniscus. As shown in (**Figures 2**-**5**), the maximum equivalent stress was significantly different between the medial condyle cartilage and the lateral condyle of the femur cartilage at 0°-90° of knee flexion ($P < 0.05$). However, the maximum equivalent stress of the lateral femoral condyle cartilage was lower than that obtained from the medial femoral condyle cartilage. The maximum equivalent stress statistically differed between the medial tibial cartilage and the lateral tibial cartilage at 0°-90° of knee flexion ($P < 0.05$). However, the maximum equivalent stress of the lateral tibial cartilage was lower than that obtained from the medial tibial cartilage. Similar results were obtained from the lateral meniscus compared with the stress of the medial meniscus.

As shown in (**Figures 6**-**9**), the maximum equivalent stress statistically differed between the medial femoral condyle cartilage and the lateral femoral condyle cartilage at 0°-90° of knee flexion. Significant differences in the femoral medial and lateral condyle cartilage, medial and lateral tibial plateau cartilage, and medial and lateral meniscus stress were noted between the two groups at a 0° angle of knee flexion ($P < 0.05$) (**Tables 3** and **4**); the increases were 64.8%, 70.9%, 83.6%, 140.9% and 24.7%, respectively (**Figure 9** and **Table 5**).

A statistically significant difference in the value of articular cartilage and meniscus stress was noted between the cartilage defect and the normal group at 30° knee flexion ($P < 0.05$) (**Figure 10** and **Table 4**).

A statistically significant difference in the value of articular cartilage and meniscus stress was noted between the cartilage defect and the normal group at 60° knee flexion ($P < 0.05$) (**Figure 11** and **Table 4**).

No significant difference in the peak strain values of the meniscus was noted in the cartilage defect group at 90° of knee flexion compared with the normal group ($P > 0.05$) (**Figure 11**).

Discussion

Exploring compressive stress and strain has been a general topic of interest in clinical

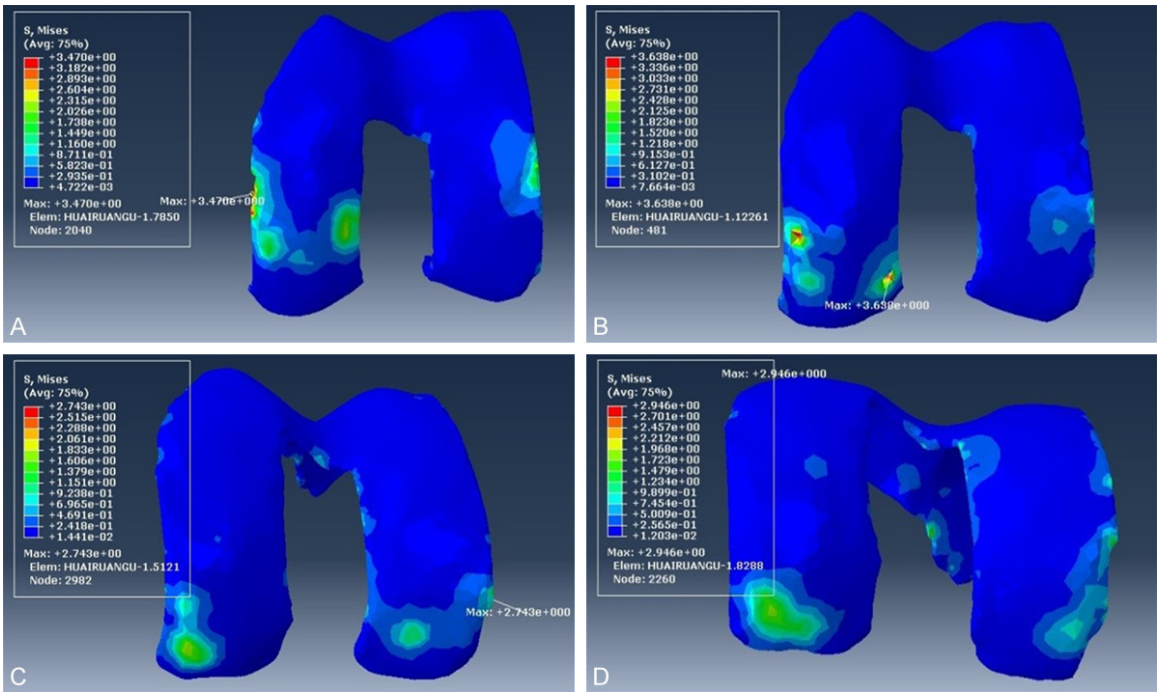

Figure 3. Von Mises stress distribution at the femoral condyle cartilage in the normal knee. A. 0° Flexion angle. B. 30° Flexion angle. C. 60° Flexion angle. D. 90° Flexion angle.

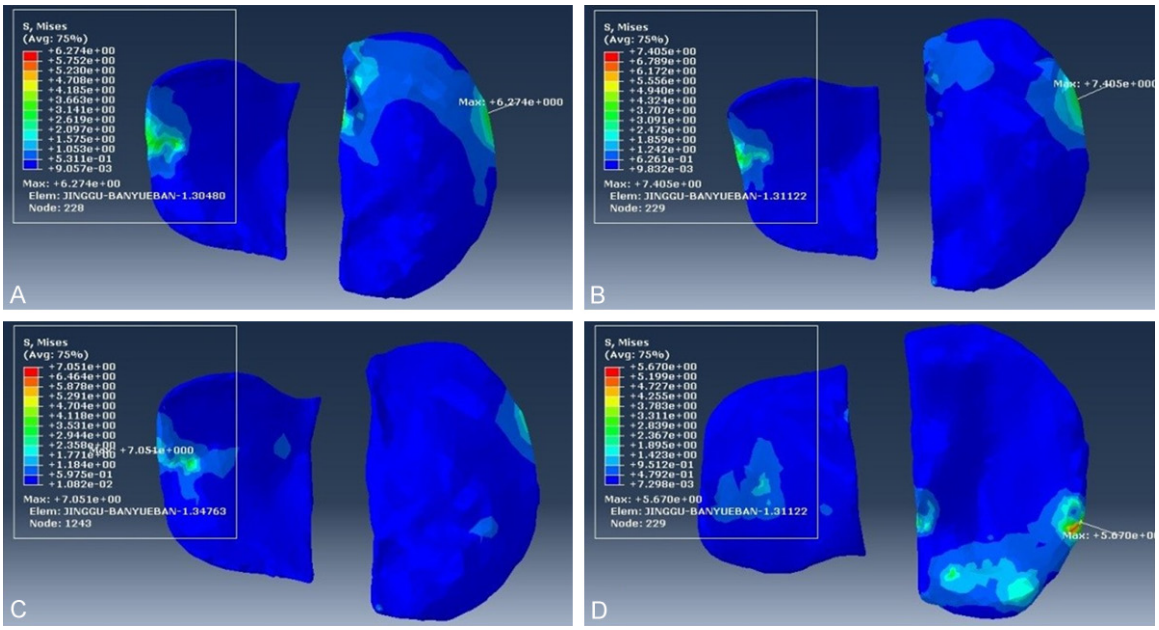

Figure 4. Von Mises stress distribution at the tibia cartilage in the normal knee. A. 0° Flexion angle. B. 30° Flexion angle. C. 60° Flexion angle. D. 90° Flexion angle.

research. However, such experimental clinical studies can be quite complex largely because the thickness and strength of the articular cartilage are different in different parts. An 8-mm defect was created in the medial femoral condyle because arthroscopy usually detects damage in this area [16-18]. Arthroscopy is currently the primary means of diagnosing and treating knee disorders.

The stability of the human knee is provided by articular cartilage, muscles, ligaments and

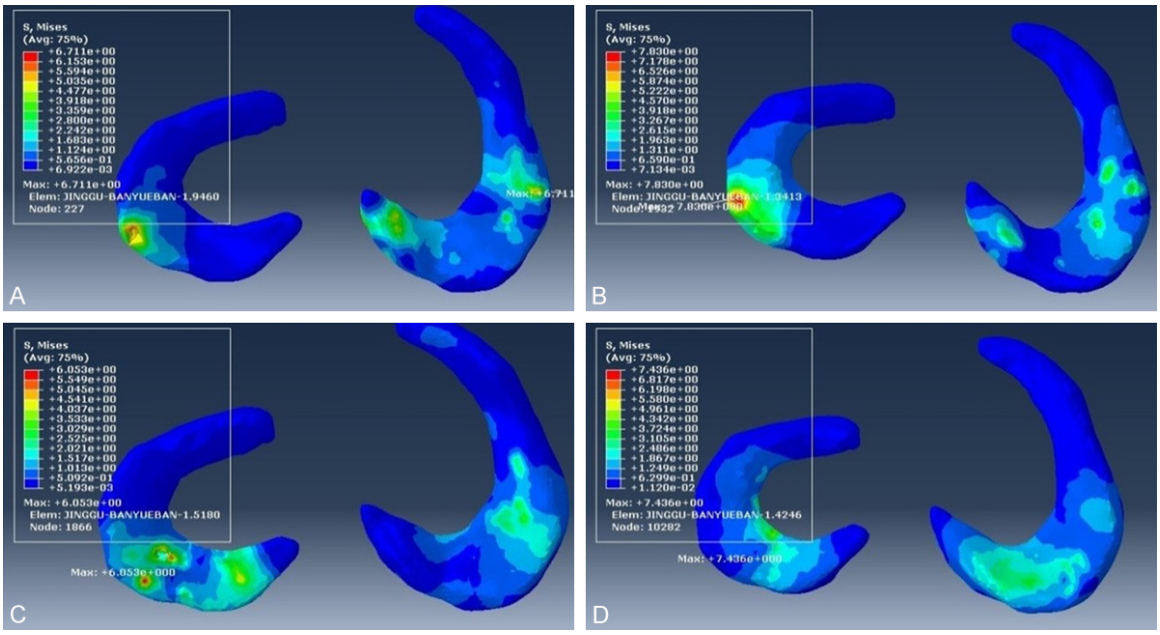

Figure 5. Von Mises stress distribution at the meniscus in the normal knee. A. 0° Flexion angle. B. 30° Flexion angle. C. 60° Flexion angle. D. 90° Flexion angle.

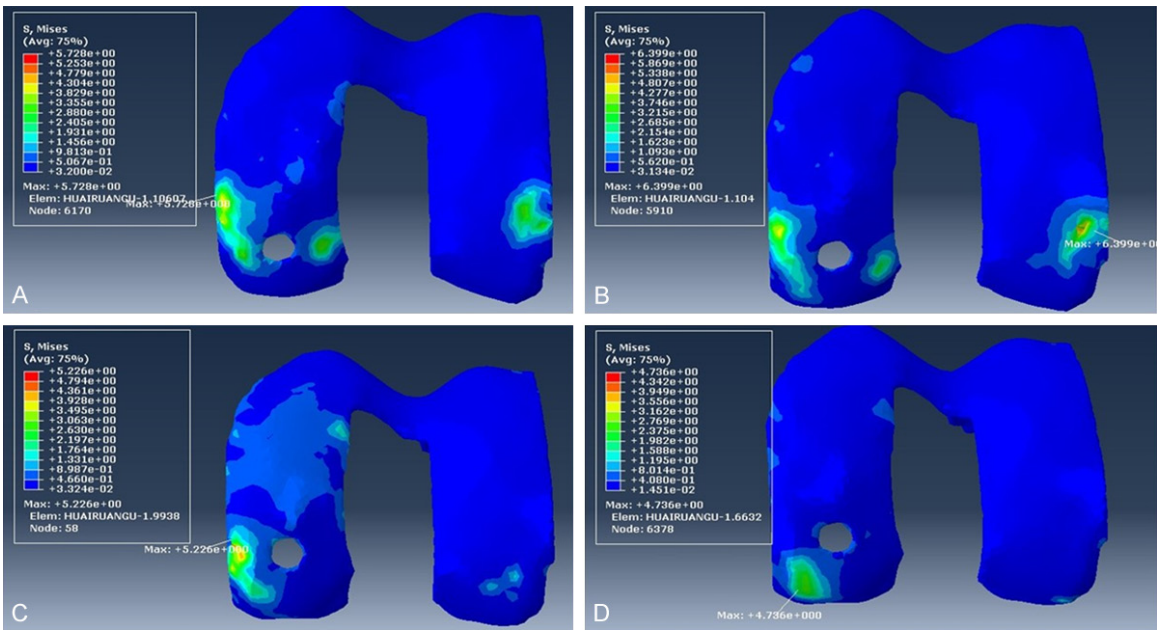

Figure 6. Von Mises stress distribution at the femoral condyle cartilage in the knee with the defect. A. 0° Flexion angle. B. 30° Flexion angle. C. 60° Flexion angle. D. 90° Flexion angle.

menisci. The structures should be reconstructed in the 3D knee joint model when performing this analysis due to their importance [19, 20]. Most of the previous 3D models did not reconstruct the surrounding ligaments and cartilage [21, 22], which led to the loss of ligament constraints on the knee during finite element analysis. Moreover, Halonen et al emphasized the importance of patella and quadriceps forces in a study of knee cartilage during a gait cycle

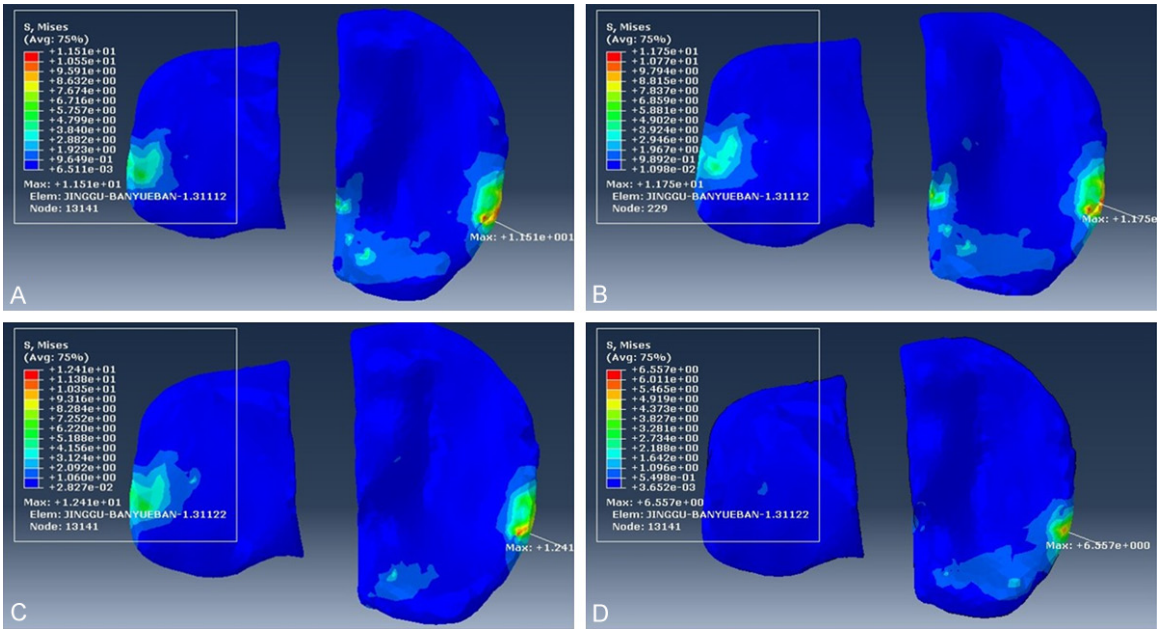

Figure 7. Von Mises stress distribution at the tibia cartilage in the knee with the defect. A. 0° Flexion angle. B. 30° Flexion angle. C. 60° Flexion angle. D. 90° Flexion angle.

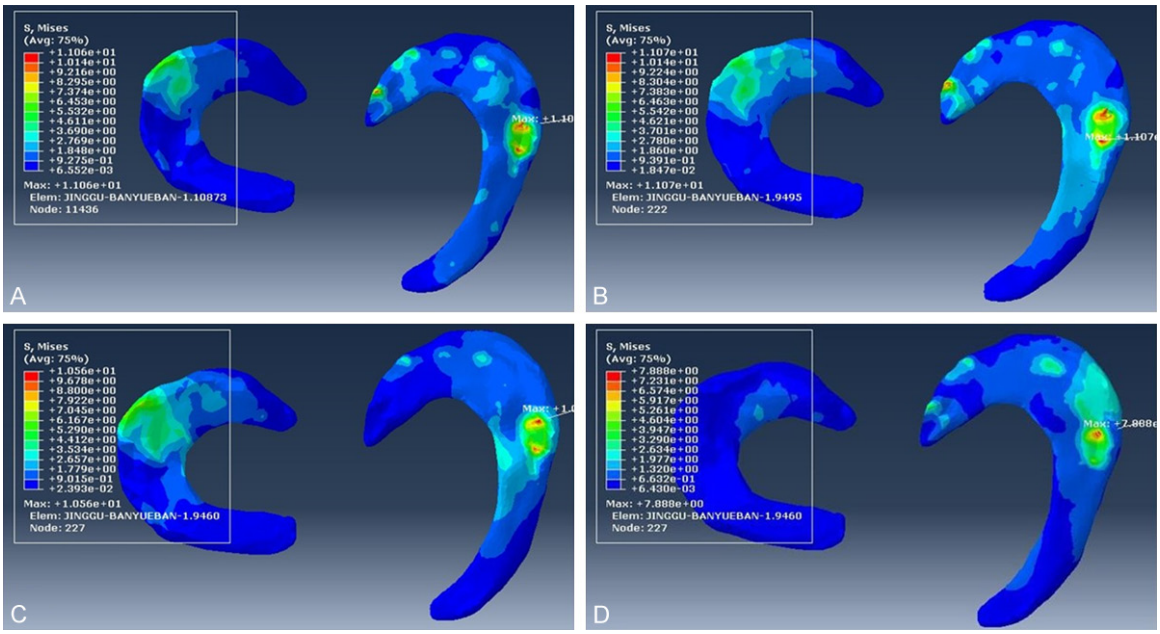

Figure 8. Von Mises stress distribution at the meniscus in the knee with the defect. A. 0° Flexion angle. B. 30° Flexion angle. C. 60° Flexion angle. D. 90° Flexion angle.

[23]. The present knee FEM was composed of 14 structures, including 5 main ligaments (the PT, ACL, PCL, MCL, and LCL). No studies have demonstrated that different joint flexion angles modify the contact variables or have investigated biomechanical changes in the knee. Peña et al. [9], Marchi et al. [24] and Dong et al. [25] analysed only the static conditions of the knee at 0° flexion. Schinhan et al showed that a 7-mm cartilage defect caused an overload of

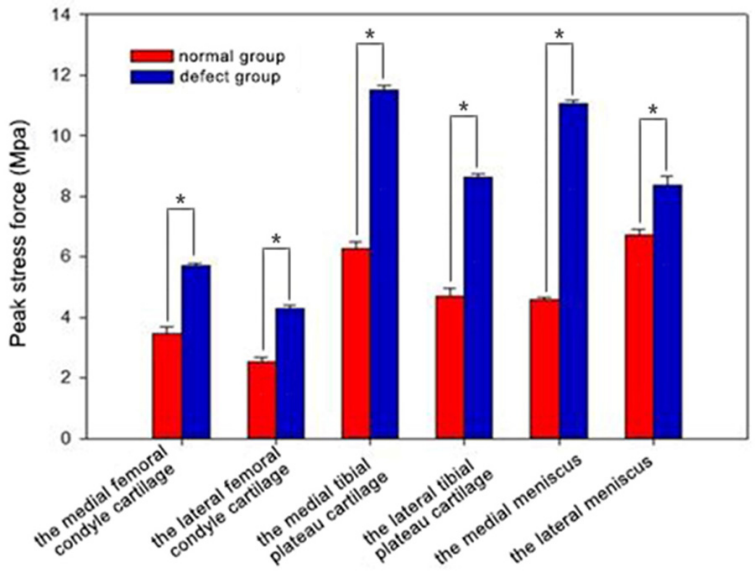

Figure 9. Histogram of the peak stress force on the articular cartilage and meniscus in the normal and cartilage defect groups at a 0° flexion angle. Asterisks indicate values that were significantly different between the groups. *P < 0.001.

the corresponding site, resulting in more severe degenerative changes in the cartilage compared with a 14-mm cartilage defect [26]. Thus, an 8-mm local full-thickness cartilage defect at the high-weight-bearing areas of the medial femoral condyle surface was selected for lesion simulations. The study sought to analyse contact variables in the articular cartilage and meniscus at 0°, 30°, 60°, and 90° of knee flexion.

The experiments in the present study simulated biomechanical changes resulting from femoral condyle cartilage defects, especially on the adjacent cartilage defects and menisci. The results obtained from Abaqus finite element analysis software indicated that the medial femoral condyle cartilage defect generated an abnormally increasing pressure surrounding the cartilage defect of the medial femoral condyle accompanied by an increase in lateral femoral condyle cartilage secondary stress. Similar results were also obtained by Shelbourne et al. [27]. Finite element analysis results indicate that the peak stress-strain zones of the femoral condyle cartilage appeared in high-weight-bearing areas at different body flexion angles. This effect was similar to that found in previous clinical studies, where the incidence of medial condyle cartilage and lateral condyle cartilage degeneration gradually increased after the medial femoral condyle cartilage was injured [9, 25, 26, 28].

The compressive stresses in the femoral cartilage, meniscus, and tibial cartilage significantly increased at 0°-30°-60° of knee flexion. The cartilage defect group at 90° of knee flexion showed no significant differences in the peak values of the meniscus compared with the normal group. Similar results were obtained by Darryl et al. and Guettler et al. [13, 29]. Darryl investigated only contact variables in the tibiofemoral joint at 0° flexion, and the location of the osteochondral defect was different from that in the present study [13]. Guettler also found that the stress in the bilateral femoral condyle and bilateral tibia plateau increased significantly at 30° of knee flexion. The maximal compressive stress in the medial compartment was higher than that in the lateral compartment in healthy groups. Similar results were obtained by Yang et al. and Carter et al. [12, 30].

Typically, the non-weight-bearing area of the tibiofemoral articular surface and the normal fluid pressure are important factors in maintaining normal articular cartilage nutrition [31]. The high contact pressures adjacent to the defect may interfere with the ability of cartilage around the defect to function normally [29, 32]. Additionally, a change in the weight-bearing area of the tibiofemoral joint can cause intra-articular synovial fluid flow barriers, leaving the affected cartilage with fewer nutrients from the synovial fluid and creating difficult for cartilage cells in obtaining sufficient water and nutrients to repair cartilage defects [31, 32]. Cristiani et al. [33] and Balazs et al. [34] confirmed that a change in the stress in the cartilage and meniscus is one of the most important factors causing cartilage degeneration and meniscus injury.

In summary, the present study investigated biomechanical changes caused by common

Table 3. The maximum Von Mises stress at the cartilage of the femoral condyle, tibial plateau and meniscus at 0°, 30°, 60°, 90°flexion angles (MPa)

	0°	30°	60°	90°
The medial femoral condyle cartilage	3.47±0.12	3.64±0.09	2.74±0.05	2.95±0.16
The lateral femoral condyle cartilage	2.51±0.07	2.21±0.02	2.60±0.01	1.96±0.15
The medial tibial plateau cartilage	6.27±0.11	7.41±0.05	7.05±0.18	5.67±0.22
The lateral tibial plateau cartilage	4.70±0.15	5.56±0.22	5.29±0.24	4.25±0.23
The medial meniscus	4.59±0.08	6.52±0.09	5.04±0.07	6.19±0.25
The lateral meniscus	6.71±0.10	7.13±0.01	6.05±0.29	7.44±0.16

Table 4. Results of the statistical analysis between the normal and defective groups

	0°	30°	60°	90°
The medial femoral condyle cartilage	< 0.001*	< 0.001*	< 0.001*	0.07
The lateral femoral condyle cartilage	< 0.001*	< 0.001*	< 0.001*	0.09
The medial tibial plateau cartilage	< 0.001*	< 0.001*	< 0.001*	0.13
The lateral tibial plateau cartilage	< 0.001*	< 0.001*	< 0.001*	0.21
The medial meniscus	< 0.001*	< 0.001*	< 0.001*	0.24
The lateral meniscus	< 0.001*	0.001*	< 0.001*	0.058

*Statistically significant (P < 0.05).

Table 5. Results of the percentage increments in the normal group with respect to the defective group

	0°	30°	60°
The medial femoral condyle cartilage	64.8%	75.8%	90.9%
The lateral femoral condyle cartilage	70.9%	95.9%	67.6%
The medial tibial plateau cartilage	83.6%	58.6%	76.0%
The lateral tibial plateau cartilage	83.6%	58%	75.9%
The medial meniscus	140.9%	72.1%	109.5%
The lateral meniscus	24.7%	30.5%	16.3%

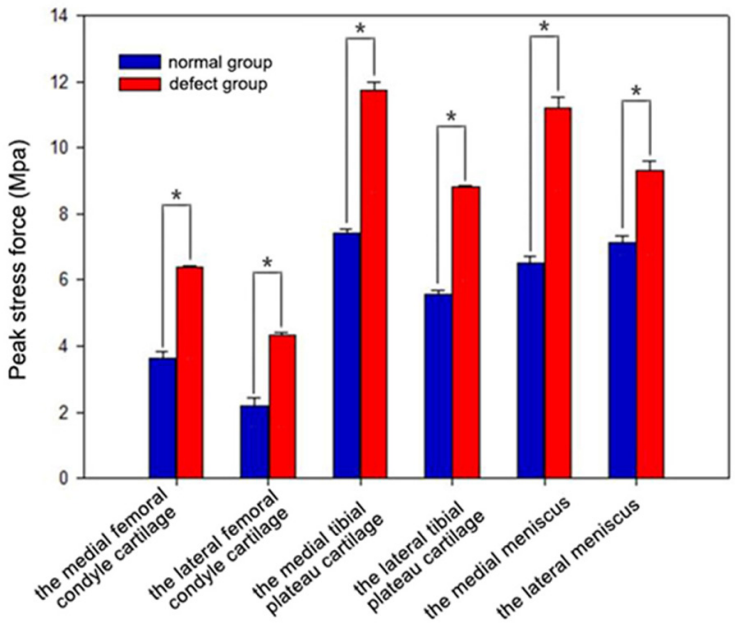

Figure 10. Histogram of the peak stress force on the articular cartilage and meniscus in the normal and cartilage defect groups at a 30° flexion angle. Asterisks indicate values that were significantly different between the groups, *P < 0.001.

osteochondral defects at 0°, 30°, 60°, and 90° of knee flexion in the presence of physiological compression forces. However, the study had several limitations. First, the model was simulated for only one size; hence, the position of osteochondral defects in degenerative joint pain was a limitation. Second, the cartilage defect had a round shape, which appears to be non-physiological in the clinical setting. Although the comparison cannot be considered a perfect model, these findings will aid in a better understanding of degenerative arthritis.

Conclusion

This study demonstrated that with an 8-mm defect in the

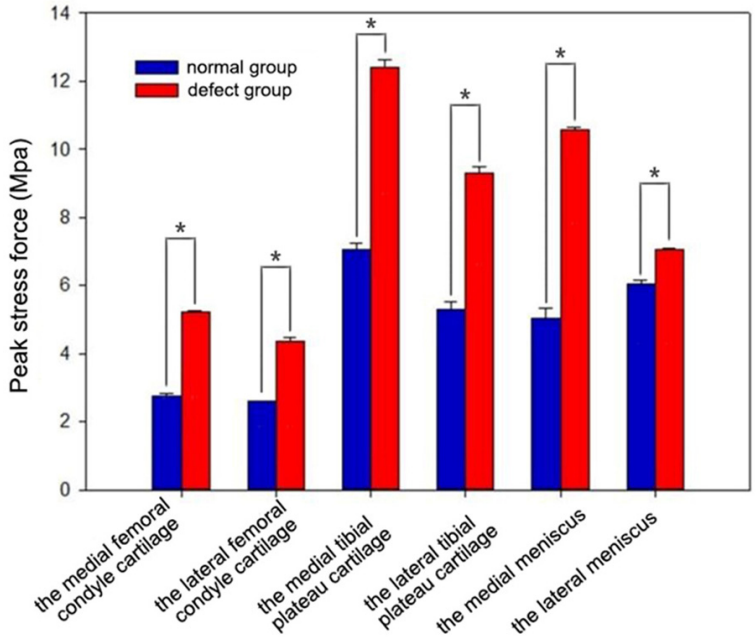

Figure 11. Histogram of the peak stress force on the articular cartilage and meniscus in the normal and cartilage defect groups at a 60° flexion angle. Asterisks indicate values that were significantly different between the groups, *P < 0.001.

medial femoral condyle at 0°, 30°, 60°, and 90° of knee flexion, the compressive stresses in the femoral cartilage, meniscus, and tibial cartilage significantly increased. Changes in stress distributions are of great significance in long-term degeneration of adjacent cartilage defects.

Acknowledgements

Innovation Team Project in Yunnan Province (No. 2014HC018) and National Cooperation Foundation of Yunnan (No. 2013IA004).

Disclosure of conflict of interest

None.

Address correspondence to: Yan-Lin Li, Department of Sports Medicine, The First Affiliated Hospital of Kunming Medical University, Kunming, China. E-mail: 852387873@qq.com

References

[1] Vannini F, Spalding T, Andriolo L, Berruto M, Denti M, Espregueira-Mendes J, Menetrey J, Peretti G, Seil R and Filardo G. Sport and early osteoarthritis: the role of sport in aetiology, progression and treatment of knee osteoarthritis. Knee Surg Sports Traumatol Arthrosc 2016; 24: 1786-1796.

[2] Filardo G, Andriolo L, Soler F, Berruto M, Ferrua P, Verdonk P, Rongieras F and Crawford DC. Treatment of unstable knee osteochondritis dissecans in the young adult: results and limitations of surgical strategies-The advantages of allografts to address an osteochondral challenge. Knee Surg Sports Traumatol Arthrosc 2019; 27: 1726-1738.

[3] Huang K, Li Q, Li Y, Yao Z, Luo D, Rao P and Xiao J. Cartilage tissue regeneration: the roles of cells, stimulating factors and scaffolds. Curr Stem Cell Res Ther 2018; 13: 547-567.

[4] Kang KT, Koh YG, Son J, Kim SJ, Choi S, Jung M and Kim SH. Finite element analysis of the biomechanical effects of 3 posterolateral corner reconstruction techniques for the knee joint. Arthroscopy 2017; 33: 1537-1550.

[5] Marchi BC and Arruda EM. A study on the role of articular cartilage soft tissue constitutive form in models of whole knee biomechanics. Biomech Model Mechanobiol 2017; 16: 117-138.

[6] Papaioannou G, Demetropoulos CK and King YH. Predicting the effects of knee focal articular surface injury with a patient-specific finite element model. Knee 2010; 17: 61-68.

[7] Cheung JT, Zhang M, Leung AKL and Fan YB. Three-dimensional finite element analysis of the foot during standing-a material sensitivity study. J Biomech 2005; 38: 1045-1054.

[8] Peña E, Calvo B, Martínez MA, Palanca D and Doblaré M. Finite element analysis of the effect of meniscal tears and meniscectomies on human knee biomechanics. Clin Biomech (Bristol, Avon) 2005; 20: 498-507.

[9] Pena E, Calvo B, Martinez MA and Doblare M. Effect of the size and location of osteochondral defects in degenerative arthritis. A finite element simulation. Comput Biol Med 2007; 37: 376-387.

[10] LeRoux MA and Setton LA. Experimental and biphasic FEM determinations of the material properties and hydraulic permeability of the meniscus in tension. J Biomech Eng 2002; 124: 315-321.

[11] Li G, Park SE, DeFrate LE, Schutzer ME, Ji L, Gill TJ and Rubash HE. The cartilage thickness distribution in the tibiofemoral joint and its correlation with cartilage-to-cartilage contact. Clin Biomech (Bristol, Avon) 2005; 20: 736-744.
[12] Yang NH, Nayeb-Hashemi H, Canavan PK and Vaziri A. Effect of frontal plane tibiofemoral angle on the stress and strain at the knee cartilage during the stance phase of gait. J Orthop Res 2010; 28: 1539-1547.
[13] D'Lima DD, Chen PC and Colwell CW Jr. Osteochondral grafting: effect of graft alignment, material properties, and articular geometry. Open Orthop J 2008; 3: 61-68.
[14] Solheim E, Krokeide AM, Melteig P, Larsen A, Strand T and Brittberg M. Symptoms and function in patients with articular cartilage lesions in 1,000 knee arthroscopies. Knee Surg Sports Traumatol Arthrosc 2016; 24: 1610-1616.
[15] Li G, Suggs J and Gill T. The effect of anterior cruciate ligament injury on knee joint function under a simulated muscle load: a three-dimensional computational simulation. Ann Biomed Eng 2002; 30: 713-720.
[16] Hjelle K, Solheim E, Strand T, Muri R and Brittberg M. Articular cartilage defects in 1,000 knee arthroscopies. Arthroscopy 2002; 18: 730-734.
[17] Bikash K, Lamichhane A and Mahara D. Prevalence of chondral lesion in knee arthroscopy. Austin J Trauma Treat 2016; 3: 1012.
[18] Jones KJ, Sheppard WL, Arshi A, Hinckel BB and Sherman SL. Articular cartilage lesion characteristic reporting is highly variable in clinical outcomes studies of the knee. Cartilage 2019; 10: 299-304.
[19] Shriram D, Kumar GP, Cui F, Lee YHD and Subburaj K. Evaluating the effects of material properties of artificial meniscal implant in the human knee joint using finite element analysis. Sci Rep 2017; 7: 6011.
[20] Kang KT, Koh YG, Park KM, Choi CH, Jung M, Shin J and Kim SH. The anterolateral ligament is a secondary stabilizer in the knee joint: a validated computational model of the biomechanical effects of a deficient anterior cruciate ligament and anterolateral ligament on knee joint kinematics. Bone Joint Res 2019; 8: 509-517.
[21] Yang N, Canavan P, Nayeb-Hashemi H, Najafi B and Vaziri A. Protocol for constructing subject-specific biomechanical models of knee joint. Comput Methods Biomech Biomed Engin 2010; 13: 589-603.
[22] Shirazi R, Shirazi-Adl A and Hurtig M. Role of cartilage collagen fibrils networks in knee joint biomechanics under compression. J Biomech 2008; 41: 3340-3348.
[23] Halonen KS, Mononen M, Jurvelin J, Töyräs J, Kłodowski A, Kulmala JP and Korhonen R. Importance of patella, quadriceps forces, and depthwise cartilage structure on knee joint motion and cartilage response during gait. J Biomech Eng 2016; 138.
[24] Marchi BC, Arruda EM and Coleman RM. The effect of articular cartilage focal defect size and location in whole knee biomechanics models. J Biomech Eng 2019.
[25] Dong YF, Hu GH, Zhang LL, Hu Y, Dong YH and Xu QR. Accurate 3D reconstruction of subject-specific knee finite element model to simulate the articular cartilage defects. Journal of Shanghai Jiaotong University (Science) 2011; 16: 620.
[26] Schinhan M, Gruber M, Vavken P, Dorotka R, Samouh L, Chiari C, Gruebl-Barabas R and Nehrer S. Critical-size defect induces unicompartmental osteoarthritis in a stable ovine knee. J Orthop Res 2012; 30: 214-220.
[27] Shelbourne KD, Jari S and Gray T. Outcome of untreated traumatic articular cartilage defects of the knee: a natural history study. J Bone Joint Surg Am 2003; 85: 8-16.
[28] Räsänen LP, Mononen ME, Lammentausta E, Nieminen MT, Jurvelin JS and Korhonen RK. Three dimensional patient-specific collagen architecture modulates cartilage responses in the knee joint during gait. Comput Methods Biomech Biomed Eng 2016; 19: 1225-1240.
[29] Guettler JH, Demetropoulos CK, Yang KH and Jurist KA. Osteochondral defects in the human knee: influence of defect size on cartilage rim stress and load redistribution to surrounding cartilage. Am J Sports Med 2004; 32: 1451-1458.
[30] Jacobs CA, Christensen CP and Karthikeyan T. Greater medial compartment forces during total knee arthroplasty associated with improved patient satisfaction and ability to navigate stairs. J Arthroplasty 2016; 31: 87-90.
[31] Venäläinen MS, Mononen ME, Salo J, Räsänen LP, Jurvelin JS, Töyräs J, Virén T and Korhonen RK. Quantitative evaluation of the mechanical risks caused by focal cartilage defects in the knee. Sci Rep 2016; 6: 37538.
[32] Dabiri Y and Li L. Focal cartilage defect compromises fluid-pressure dependent load support in the knee joint. Int J Numer Method Biomed En 2015; 31: e02713.
[33] Cristiani R, Rönnblad E, Engström B, Forssblad M and Stålman A. Medial meniscus resection increases and medial meniscus repair preserves anterior knee laxity: a cohort study of 4497 patients with primary anterior cruciate ligament reconstruction. Am J Sports Med 2018; 46: 357-362.
[34] Balazs GC, Greditzer HG 4th, Wang D, Marom N, Potter HG, Marx RG, Rodeo SA and Williams RJ 3rd. Ramp lesions of the medial meniscus in patients undergoing primary and revision ACL reconstruction: prevalence and risk factors. Orthop J Sports Med 2019; 7: 2325967119843509.